

First-principles predictions of tunable half metallicity in zigzag GaN nanoribbons with possible applications in CO detection and spintronics

Rachana Yogi¹, Kamal K. Jha², Alok Shukla¹ and Neeraj K. Jaiswal*

September 8, 2022

¹ Department of Physics, Indian Institute of Technology Bombay, Powai, Mumbai 400076 India.

² Indian Institute of Information Technology, Vadodara, Gujarat 382028 India.

*2D Materials Research Laboratory, Indian Institute of Information Technology Design & Manufacturing, Jabalpur, M.P. 482005, India.

E-mail: neeraj@iiitdmj.ac.in

Abstract

Based on systematic first-principles density-functional theory (DFT) simulations, we predict that the zigzag GaN nanoribbons (ZGaNNR) can be used both as highly efficient CO detectors as well as spin filters. Our calculations, performed both on infinitely long nanoribbons, and also on finite strands, suggest that: (a) CO binds strongly at the edges of ZGaNNRs, and (b) that several of the resultant configurations exhibit half-metallic behavior. We considered various edge-passivation sites and found that all the resultant structures are thermodynamically stable. The metallic, half-metallic, and semiconducting configurations are observed as a function of CO passivation coverage. We also compute the current-voltage (I-V) characteristics of various structures using the Landauer formalism, and find that the devices made up of half-metallic configurations act as highly-efficient spin filters. The effect of CO concentration is also investigated which suggests a viable way to not just tune the electronic band gap of ZGaNNRs, but also their half metallicity. Our simulations thus suggest a new direction of research for possible device applications of III-V heterostructures.

• **Keywords:** Nanoribbons, Gallium Nitride, Zigzag, Carbon monoxide, detection/capturing, spin filtering.

Introduction

2-D materials [1, 2, 3, 4] exhibit potential candidature as a building block in upcoming sensing devices due to their higher surface to volume ratio, unique electron confinement and mature synthesis techniques compared to their 1-D counterparts [5, 6, 7, 8, 9, 10]. Their outstanding electronic, magnetic and transport properties, higher carrier mobility also makes them center of attraction for various technological applications [11, 12, 13, 14, 15, 16, 17, 18, 19]. It is reported that nanoribbons can be realized either by cutting [20] mechanically exfoliated nanosheet [21] or by patterning epitaxially grown nanosheet [22, 23]. The obtained nanoribbons are in the form of zigzag, armchair and chiral [24, 25, 26]. Edge shape play a vital roll in case of nanoribbons as all the electronic, magnetic and transport properties are significantly influenced by their edge geometries [27, 28, 29, 30, 31, 32, 26]. GaN nanoribbons are successfully synthesized using various technique [33, 34, 2, 35]. The electronic and magnetic properties of nanoribbons make them a good candidate for various applications [36].

Continuous advancement in industries and growth of traffic increases the pollution rate day by day. Therefore, the development of highly efficient sensors is one of the most active area of research nowadays. The exceptional electronics properties and edge reactivity of 2D material makes them a good candidate for detection of gas molecule at very low concentration [37, 38, 39, 40]. GaN nanoribbons exhibit wide band gap and a promising material for optoelectronic and high power applications. On the other hand, its investigations towards sensing devices are very limited [41, 10, 42]. The application of GaN in sensing devices could be superior compared to graphene which

is restricted via zero band gap behavior [43, 44]. As CO is one of the most common environment pollutant gas, it is highly warranted to develop CO sensing/capturing devices in near future. On the other hand, the intrinsic wide band gap of GaNNR could obstruct its path for semiconducting device applications. The interaction of CO with GaNNR edges may affect their electronic properties. Therefore, the present study, CO passivation with GaN based zigzag nanoribbons (ZGaNNR) is investigated towards possible CO detection and its effect on the band gap modulation. In our study we focused on the electronic behavior of the material through which we have also analyzed the charge transfer due to the passivation of gas molecule on ZGaNNR. Typically, the charge transfer to the molecule or from the molecule, also induces change in electric resistivity of the material.

Model and Methodology

The present investigations were performed using first-principles self-consistent calculations based on density functional theory (DFT). We used QuantumATK DFT code [45] for the present simulation results. The generalized gradient approximation (GGA) in the form of Perdew-Burke-Ernzerhof (PBE) was used as exchange correlation potential [46]. The considered configurations of ZGaNNR were modelled with periodic boundary conditions having repetition along Z-axis whereas X and Y directions were kept confined. The norm-conserving pseudo-potential with 70 Ry energy mesh cut-off value was adopted to define the fineness of the grid. Further, double ζ polarized basis set has been considered for all constituent atoms. The Monkhorst-Pack Grid [47] for k-point sampling was selected as $1 \times 1 \times 50$ for defining the sampling of the Brillouin zone centered at Γ . To avoid inter-ribbon interactions, ribbons were separated using a cell padding vacuum of 10\AA along the confined directions. During the geometry optimization, we used Pulley mixer algorithm with $1 \times 10^{-5} \text{ Ry}$ tolerance for self-consistent iteration loop and all the atoms were free to change their positions during optimization to attain the minimum energy configuration. The geometries were relaxed without any constraint till the force and stress on each atom reduces to a criterion of 0.05 eV/\AA and 0.05 eV/\AA^3 respectively. The ribbon width is defined in the conventional manner *i.e.* the number of Ga-N bonds across the transverse direction [48, 49]. Five different passivation sites on ZGaNNR are considered for CO molecule as illustrated in Fig. 1.

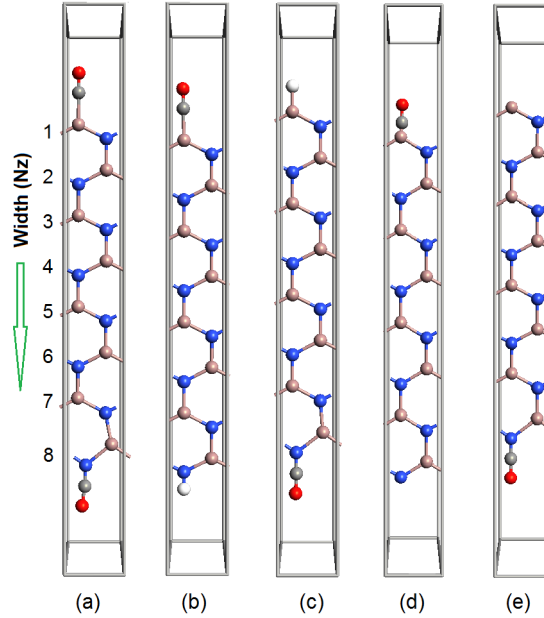


Figure 1: The schematics of zigzag GaN nanoribbon with passivation of CO on (a) CO-ZGaNNR-CO, (b) CO-ZGaNNR-H, (c) H-ZGaNNR-CO, (d) CO-ZGaNNR and (e) ZGaNNR-CO at width-8.

Table 1: Calculated bond lengths and bond angles of CO passivated zigzag GaN nanoribbons

ZGaNNR	
Bond length (Å)	Bond angle (°)
C-O = 1.81 (Ga edge)	$\angle CGaN = 116.39$ (Ga edge)
C-O = 1.19 (N-edge)	$\angle GaNGa = 116.87$ (Ga edge)
C-Ga = 1.90	$\angle HGaN = 118.08$ (Ga edge)
Ga-N = 1.86	$\angle CNGa = 131.20$ -126.58 (N-edge)
Ga-H = 1.53	$\angle NGaN = 118.10$ (N-edge)
C-N = 1.25	$\angle HNGa = 115.73$ (N-edge)
N-H = 1.25	

Results and discussion

Structural Stability

To find out the most suitable passivation sites, various possible configurations have been modeled. It is noticed that bonding of CO molecule with the GaN nanoribbons takes place via C side as shown in Fig. 1. The variation in bond length and bond angle has been illustrated in Table 1. To avoid an ambiguity, the structural stability of CO passivated GaN nanoribbons is further discussed in separate subsections for ZGaNNR.

The reported lattice constant of zigzag GaN nanoribbon is 3.18Å which shows good agreement with our results (3.32Å)[50]. All the properties of nanoribbons are highly dependent on their edge shape and ribbon width. First we investigate the structural stability of bare and H-passivated nanoribbons.

 Table 2: Variation of adsorption energy (E_{ad}), binding energy (BE), band gap (E_g) and Fermi energy (E_F) of H-passivated and bare zigzag GaN nanoribbons as a function of ribbon width.

Width (N_Z)	ZGaNNR (eV)					
	H-Passivated			Bare		
	E_{ad}	E_g	E_F	BE	E_g	E_F
4	-5.65	3.40	-3.17	-5.83	M	-4.96
6	-5.69	3.04	-3.55	-6.02	M	-4.99
8	-5.70	2.86	-3.68	-6.12	M	-4.98

To insure the structural stability we have calculated the binding energy (BE) for bare ribbons and adsorption energy for H-passivated ribbons respectively and the calculated values are depicted in Table 2. To calculate the BE following relation has been used [51, 52]:

$$BE = \frac{1}{m+n} [E_{total} - m(E_{Ga}) - n(E_N)] \quad (1)$$

where E_{total} , E_{Ga} and E_N are, the total energies of bare ribbon, isolated Ga, and N atom. Similarly, m and n represented the number of Ga and N atoms in the nanoribbon respectively. As per the definition adopted here, negative binding or adsorption energy exhibits exothermic nature while the magnitude signifies thermodynamic stability. It is noticed that structural stability increases with the ribbon width. To find the most stable CO passivated nanoribbon, we calculate adsorption energy (E_{ad}) of considered configurations including H passivation. The following relation has been utilized for E_{ad} calculation: [53, 54]

$$E_{ad} = \frac{1}{n} [E_T - E_{bare} - nE_{H/CO}] \quad (2)$$

where E_T , E_{bare} , $E_{H/CO}$ are the total energies of considered configuration after attachment of CO/H, bare nanoribbon, isolated CO molecule/H atoms, respectively and n is number of passivated molecules/atoms.

Table 3: Variation of adsorption energy (E_{ad}), Fermi energy (E_F) and band gap (E_g) of zigzag GaN nanoribbons with CO passivation as a function of ribbon width.

Configurations	Width (N_Z)	E_{ad} (eV)	E_F (eV)	Eg (eV)	
				Spin up	Spin down
CO-ZGa _N -CO	4	-1.64	-3.44	M	0.5
	6	-1.66	-3.41	M	0.5
	8	-1.71	-3.51	M	0.6
CO-ZGa _N -H	4	-3.67	-3.06	M	3.0
	6	-3.71	-3.05	M	2.6
	8	-3.71	-3.04	M	2.5
H-ZGa _N -CO	4	-3.64	-3.43	2.5	1.0
	6	-3.68	-3.53	2.1	0.9
	8	-3.69	-3.64	2.0	0.9
CO-ZGa _N	4	-1.19	-4.49	M	M
	6	-1.20	-4.44	M	M
	8	-1.75	-4.81	M	M
ZGa _N -CO	4	-2.65	-3.51	1.0	0.2
	6	-2.69	-3.55	0.9	0.2
	8	-2.68	-3.63	0.8	0.2

For sensing of CO molecules, five different passivation sites are considered as illustrated in Fig. 1. The structural stability of all considered geometries of ZGaNNR are tabulated in Table 3. The magnitude of adsorption energy is much higher than thermal excitation energy (≈ 25 meV) which suggests that all the configurations are thermally stable. Interestingly, it is also noticed that the most energetically favorable configuration is CO-ZGa_N-H followed by H-ZGa_N-CO from which we conclude that the presence of passivating H atoms effectively increases the stability of ZGa_N nanoribbon. Similarly, the order of least favorable configurations are CO-ZGa_N, CO-ZGa_N-CO and ZGa_N-CO. The Fermi energy also varies as the ribbon width increases. In all the configurations the Fermi level shifts in downward direction with respect to its bare counterpart. The downward shifting of Fermi level is analogous to p-type doping candidature. It is also concluded that after passivation of CO, ZGa_N nanoribbons are stable in antiferromagnetic (AFM) ground state. We tried to incorporate the effect of vdW corrections however, there was no change in the ground state energy of the structures. This is due to the reason that all the adsorbed CO molecules form stable chemical bonds with the host nanoribbons. Therefore, the weak physical interactions are not affecting the ground state of the system [55, 56].

Electronic properties

The electronic band structures of ZGaNNR with passivation of CO on the edges of nanoribbon are illustrated in Fig. 2. It is reported that zigzag bare GaNNR is metallic in nature whereas H-passivation exhibits a band gap [42, 57]. Also, zigzag bare and H-passivated GaNNR, both are stable in non-magnetic ground states, respectively. It is revealed that presence of CO on the edges of ZGaNNR profoundly affects the electronic properties of ZGaNNR. After passivation of CO, ZGaNNR is stable in AFM ground state. The observed AFM ground state could be further explained on the basis of electronegativity difference between C and the host edge atoms (Ga and N). The electronegativity of C is greater (smaller) than the Ga (N) atoms. Owing to this, an unequal charge transfer takes place between the adsorbed CO molecule and the edge Ga/N atoms. It creates a difference between the electric potentials of the opposite edges which in turn favors the AFM ground state. Similar magnetic behavior has been previously reported for graphene nanoribbons functionalized with different atoms/groups [58]. Interestingly, when both edges of nanoribbon are containing CO molecule [Fig. 1] and when CO is passivated on the Ga edge and N edge posses H atom [Fig. 1(b)] then half metallic nature is noticed as depicted in Fig. 2 (b). Another important thing we have observed is the pure metallic character when CO is located at the Ga edge of the ribbon [Fig. 2 (d)]. However, when Ga edge is passivated by H atom or left bare, finite band gap is observed [Fig. 2 (c) and (e)]. The calculated band gap is 2.0 eV for spin-up carrier whereas 0.9 eV for spin-down charge carries of H-ZGa_N-CO configuration at ribbon width-8. Similarly, ZGa_N-CO configuration posses band gap [0.8 eV (spin-up) and 0.2 eV (spin-down)]. It is reported that H-passivated ZGaNNRs exhibit indirect band gap [57] and after passivation of CO the behavior remains same [Fig. 2 (c) and (e)].

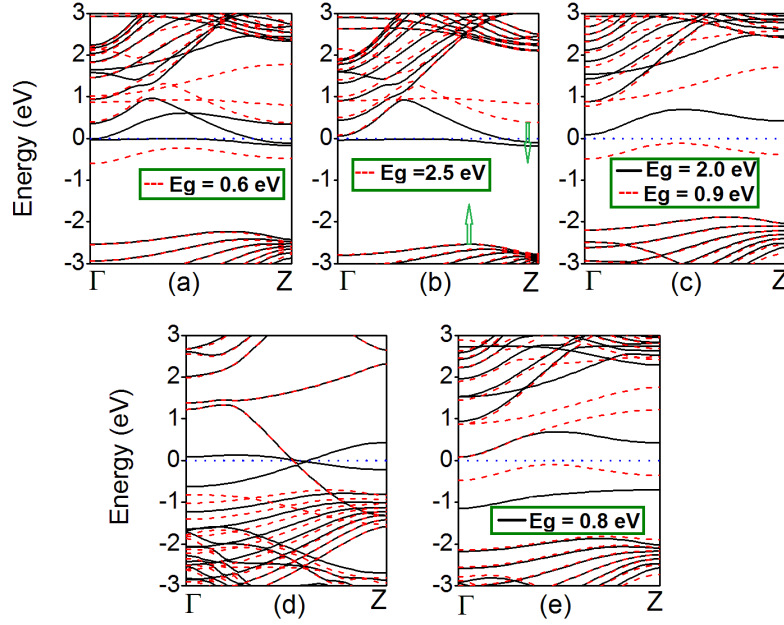


Figure 2: The spin polarized band structure of zigzag GaNNR with CO passivation for (a) CO-ZGaNNR-CO, (b) CO-ZGaNNR-H, (c) H-ZGaNNR-CO, (d) CO-ZGaNNR and (e) ZGaNNR-CO at width-8. The solid (black) and dashed (red) lines correspond to electronic states of spin up (majority spin) and spin down (minority spin) electrons respectively. The horizontal dotted line at 0 eV represents the Fermi level.

For the further understanding of electronic properties of ZGaNNR with CO passivation, we have also calculated the density of states (DOS) of all the considered geometries [Fig. 3]. It is revealed that the DOS profile exhibits good compatibility with band structure results. The similar half metallic character is also noticed in DOS of CO-ZGaNNR-CO and CO-ZGaNNR-H configurations. Similarly, the absence of energy states near the Fermi level is witnessed in H-ZGaNNR-CO and ZGaNNR-CO configuration, whereas the DOS of CO-ZGaNNR clearly exhibits metallic behavior.

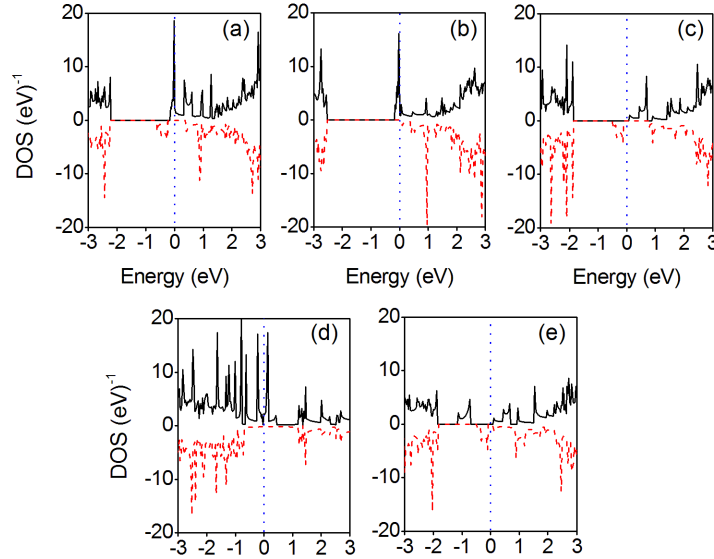


Figure 3: The spin polarized DOS of zigzag GaNNR with CO passivation for (a) CO-ZGaNNR-CO, (b) CO-ZGaNNR-H, (c) H-ZGaNNR-CO, (d) CO-ZGaNNR and (e) ZGaNNR-CO at width-8. The solid (black) and dashed (red) lines correspond to electronic states of spin up (majority spin) and spin down (minority spin) electrons respectively.

In realistic devices, there will be finite fragments of nanoribbons between the electrodes, unlike the infinitely

long structures considered for computing the band structure. Therefore, we have also investigated the electronic properties of finite fragments of CO-ZGaNNR-CO consisting of five unit cells (repetitions) as illustrated in Fig.4. Our calculations reveal that even this finite fragment exhibits half-metallic character with a finite band gap for spin down electrons ($E_g = 0.55\text{eV}$), and a negligible one ($E_g = 0.06\text{ eV}$) for spin up electrons. Hence, only the spin-up electrons will participate in conduction, leading to a spin-polarized current.

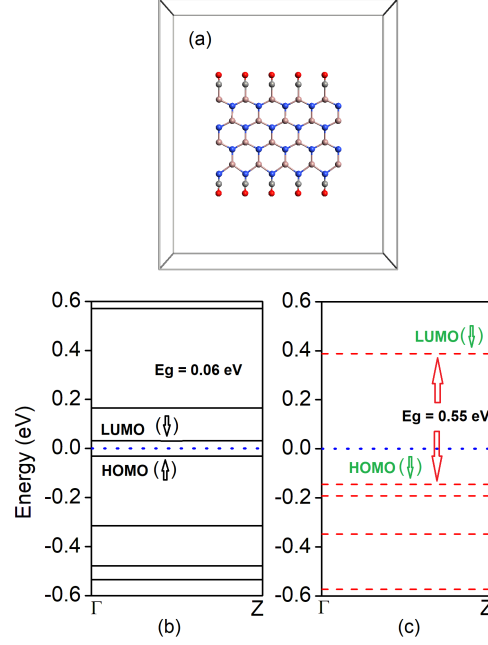


Figure 4: Energy levels of up- (b) and down-spin (c) electrons for the CO-ZGaNNR- CO fragment consisting of five repeat units (a). The solid (black) and dashed (red) lines correspond to electronic states of spin up (majority spin) and spin down (minority spin) electrons respectively. The blue dotted line at 0 eV represents the Fermi level.

For further verification of the observed half-metallic character and understanding the splitting of electronic states around the Fermi level, Bloch states have been analysed. We elected the highest valence band and the lowest conduction band for this (Bloch) analysis as these are mainly responsible for governing the electronic transport in the material. The spin polarized Bloch states for CO-ZGaNNR-CO are depicted in Fig. 5. Perusal of this figure reveals that different spins are populated at opposite edges of the ribbon. The localized behavior of electrons is also be noticed in Fig. 5 (a)-(d). Additionally, there exists a phase change of π between spatially separated charges on the two edges, further confirming the AFM ordering in the system.

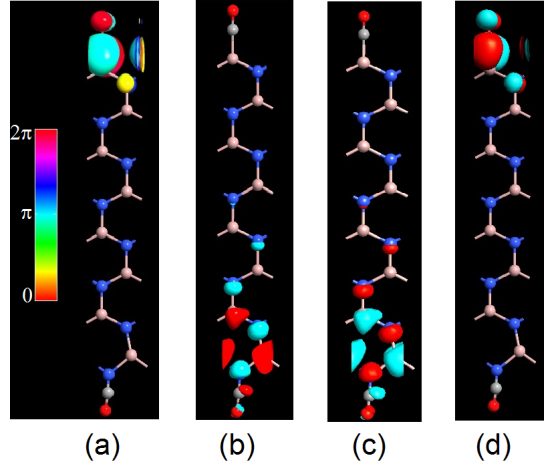


Figure 5: The computed Bloch states for highest valence band (HVB) and the lowest conduction band (LCB), plotted along the width for (a) HVB-up spin (b) HVB-down spin (c) LCB-up spin and (d) LCB-down spin.

Transport Properties

The two-probe model is used for transport [59] studies as shown in Fig 6. The calculated I-V characteristic of ZGaNNR containing CO are illustrated in Fig 7.

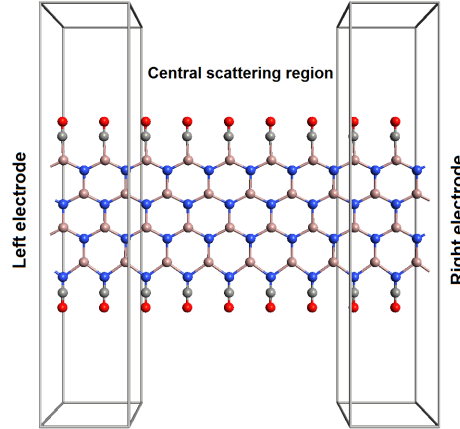


Figure 6: The Schematic diagram of the two probe geometry of ZGaN nanoribbon with CO passivation for CO-ZGaN-CO at width-5 and repetition 5 along Z axis. The nature of the device is identical for other structures (Fig 1).

It is revealed that CO-ZGaN configuration exhibits maximum current followed by CO-ZGaN-CO. In these two structures, current increases linearly upto ~ 0.6 V beyond which it starts to saturate. In contrast, an interesting behavior is noticed for rests of the other I-V characteristics. For H-ZGaN-CO, the current remains zero for entire bias window as the corresponding band gap is significantly larger (2.5 eV) than applied biasing. For remaining three structures, the current initially increases and attains a maximum value ($\sim 14 \mu A$ for bare/CO-ZGaN-H and $\sim 11.6 \mu A$ for ZGaN-CO) around 0.5 V. As the biasing is further increased, the current starts to decline and approaches 0 near 1 V. Thus, a clear signature of negative differential resistance (NDR) phenomena is obtained in these three structures.

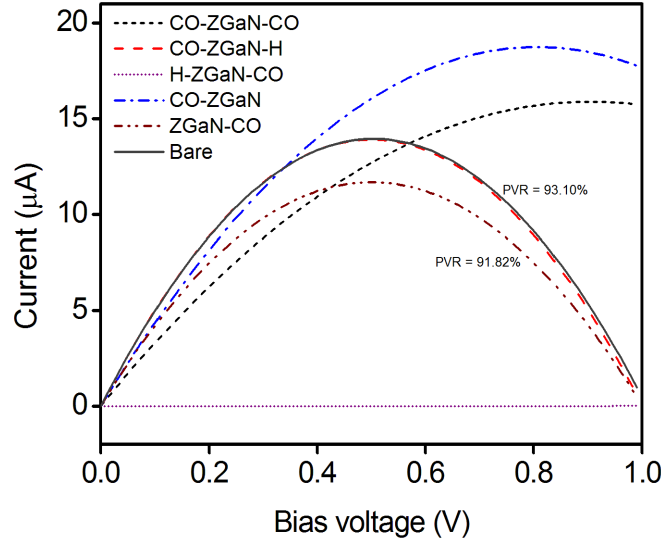


Figure 7: The calculated I-V characteristic of bare and CO passivated ZGaN nanoribbons with higher peak to valley ratio (PVR).

The observed I-V characteristics could be further understood on the basis of transmission spectra as shown in Fig 8. For CO-ZGaN and CO-ZGaN-CO, the transmission coefficient is found to be maximum (*i.e.* 4) which supports highest current in these structures. For the structures showing NDR behavior, a relatively small but finite transmission coefficient is noticed around the Fermi level. Upon increasing the biasing, reduction in the transmission takes place which is responsible for the observed NDR phenomenon.

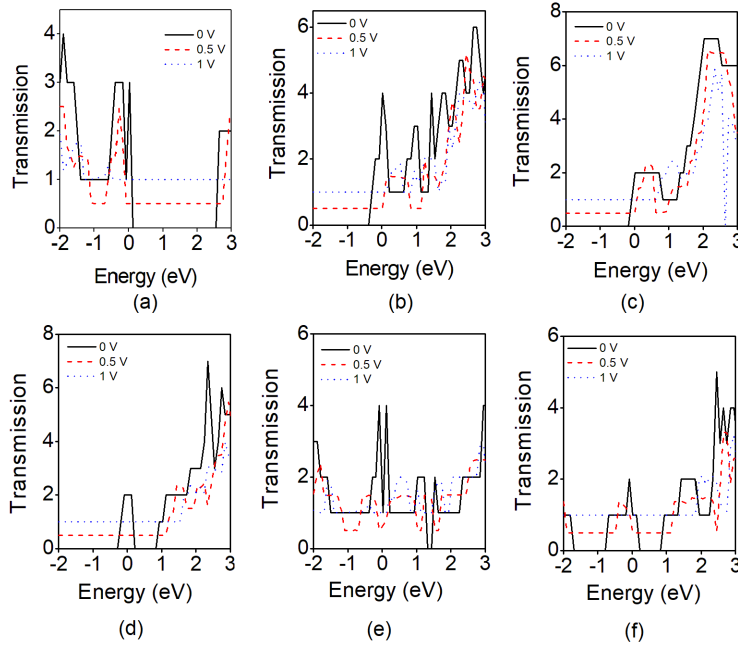


Figure 8: The calculated transmission spectra of CO passivated ZGaN nanoribbons for (a) bare, (b) CO-ZGaN-CO (c) CO-ZGaN-H, (d) H-ZGaN-CO, (e) CO-ZGaN and (f) ZGaN-CO.

To further confirm the half metallic behavior in selected structures as observed in the band structures [Fig. 2 (a), (b)], we computed spin polarized I-V characteristics. Fig 9 depicts the spin dependent currents for CO-ZGaN-CO and CO-ZGaN-H structures. It is clearly visible in both of these images that the entire current conduction takes place only due to spin up (majority spin) electrons. As the current due to spin down (minority spin) electrons remains essentially zero, it confirms the observed HM property of these structures.

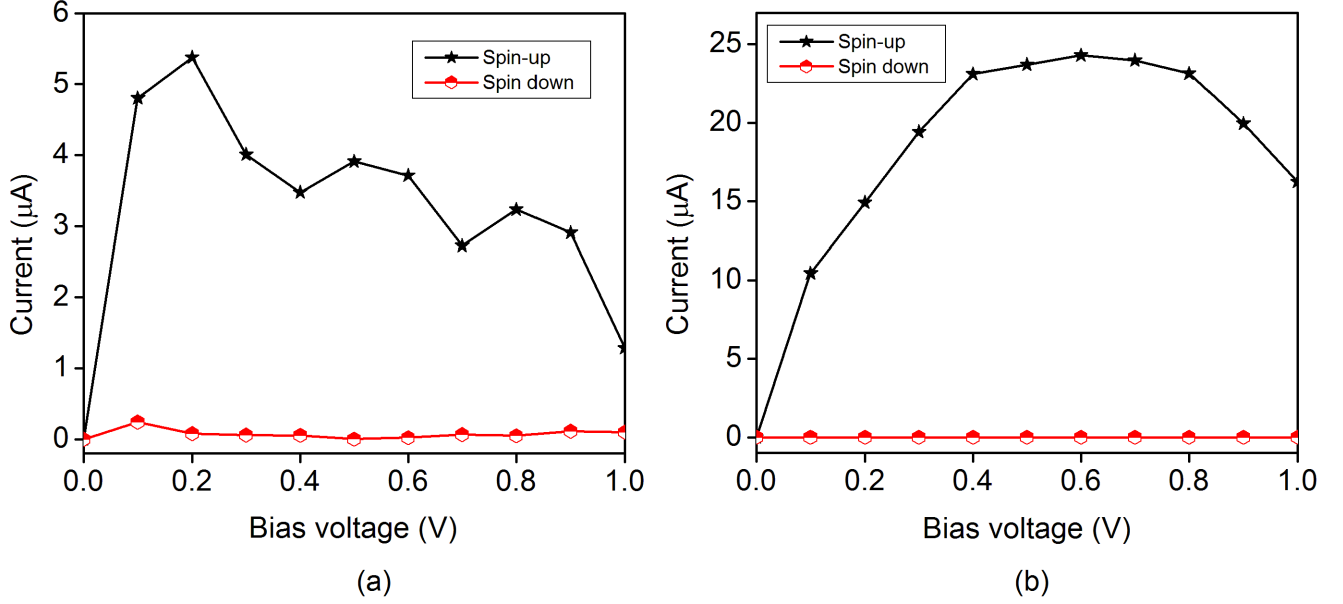


Figure 9: The calculated spin oriented I-V characteristic of CO passivated ZGaN for (a) CO-ZGaNNR-CO and (b) CO-ZGaNNR-H nanoribbons.

Spin filtering efficiency

The spin I-V characteristics of considered structures exhibit interesting features. We find that for a given voltage, the magnitude of the current due to one spin orientation is much more than that due to the other. This imbalance between the current contributed by the two different spin orientations is an important parameter for spin filtering device applications. The ability of a material or a device to select a particular spin direction can be quantified in terms of spin filtering efficiency (S_{FE}) defined as [60, 61, 62]:

$$S_{FE} = \frac{I_{spin\uparrow} - I_{spin\downarrow}}{I_{spin\uparrow} + I_{spin\downarrow}} \times 100\% \quad (3)$$

where, $I_{spin\uparrow}$ and $I_{spin\downarrow}$ are the magnitudes of the currents for spin-up and spin-down electrons, respectively. Fig 10 shows the behavior of spin filtering efficiency as a function of applied voltage for CO-ZGaNNR-CO and CO-ZGaNNR-H structures. With respect to the applied bias voltage, we note the following trends: (a) for CO-ZGaNNR-CO, S_{FE} varies in the range 86%-100%, while (b) for CO-ZGaNNR-H, S_{FE} stays constant at 100%. This behavior is fully consistent with the variation of the currents of the two spin orientations, with the applied bias voltage, for the two types of nanoribbons (see Fig 9). These results suggest that if one is looking for a perfect spin filter, CO-ZGaNNR-H is a strong candidate for the purpose.

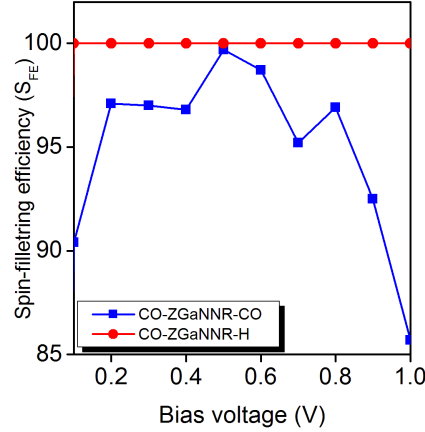


Figure 10: The calculated spin filtering efficiencies of CO-ZGaNNR-CO and CO- ZGaNNR-H.

Different CO concentration

In the present work we have also study the different CO concentration effect on the of most energetically favorable configuration (CO-ZGaN-H). Different edge coverage (0% to 100% with interval of 25%, where 0% means absence of CO and 100% means all edges are passivated by CO molecule.) of CO is obtained for the analysis of the electronic properties of CO-ZGaN-H (Fig 11).

It is noticed that the different edge coverage of CO profoundly alter the electronic properties of considered structures. The band structures of CO-ZGaN-H with different CO concentrations is illustrated in Fig 12. Interestingly, it is noticed that as the edge coverage of CO increases, the band gap decreases. The magnitude of obtained band gap is 1.5 eV (spin-up) & 1.9 eV (spin-down), 1.5 eV (spin-up) & 1.1 eV (spin-down), 0.9 eV (spin-up) & 2.1 eV (spin-down), metallic (spin-up) & 1.1 eV (spin-down), and metallic eV (spin-up) & 2.6 eV (spin-down) for 0%, 25% and 50% CO coverage. In contrast, for 75% and 100% CO coverage, the half metallic behavior is obtained as already discussed in the previous section. Thus, variation in the CO coverage could be a potential way to tailor the electronic band gap of ZGaNNR.

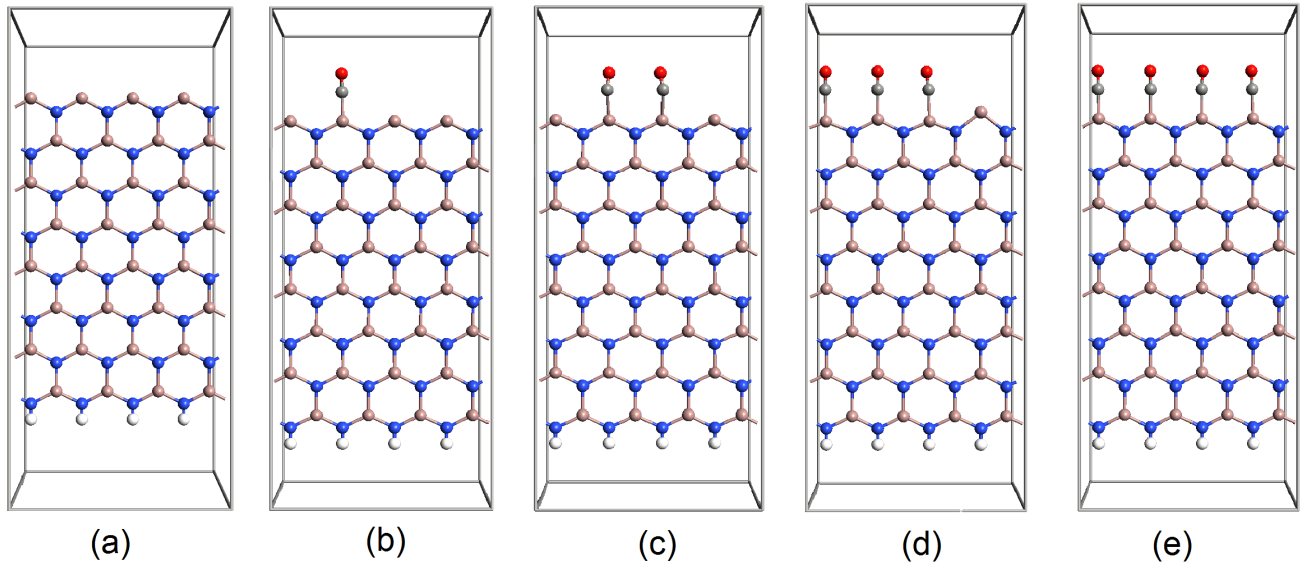


Figure 11: The Schematic diagrams of different concentration of CO on most energetically favorable configuration CO-ZGaN-H for (a) 0%, (b) 25%, (c) 50%, (d) 75% and (e) 100% at width-8 and 4 repetition.

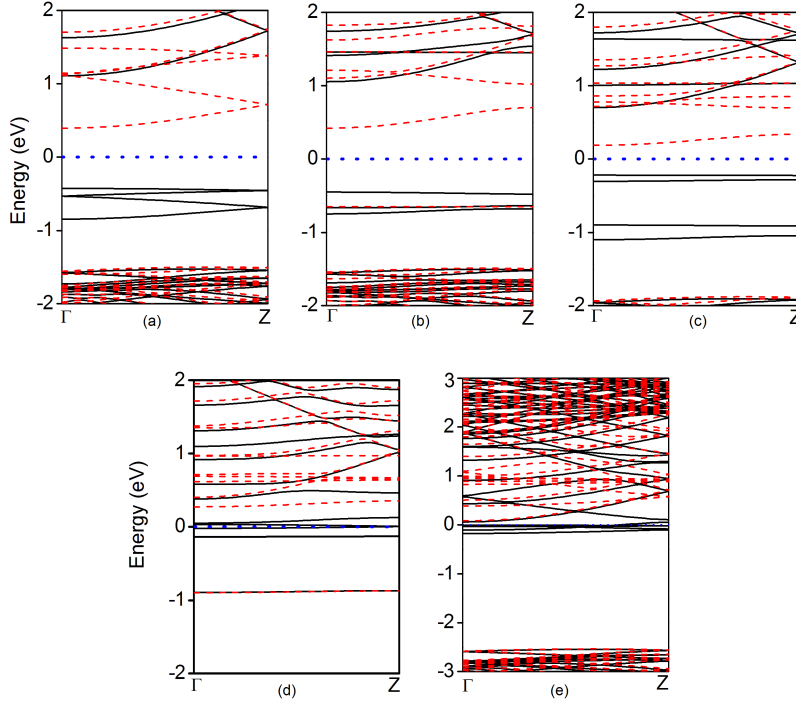


Figure 12: The calculated electronic band structure of different concentration of CO on most energetically favorable configuration CO-ZGaNNR-H for (a) 0%, (b) 25%, (c) 50%, (d) 75% and (e) 100% at width-8 and 4 repetition.

Conclusion

In summary, our DFT based first-principles calculations demonstrate that after passivation of CO molecule on one or both the edges of ZGaNNR, the nanoribbons exhibit metallic to half metallic character. Of the two possible CO-passivated configurations, we find that the nanoribbons passivated with CO on one edge (CO-ZGaNNR-H) are not only more stable as compared to the ones passivated with it on both the sides (CO-ZGaNNR-CO), but also they exhibit better spin-filtering efficiency. Furthermore, we also observe variations in Fermi energy as a function of passivation, suggesting that the edge passivation can also be used to achieve doping in these systems. The negative differential resistance observed in these structures also suggests their possible applications in fabricating oscillators and amplifiers. Therefore, we believe that structures can be used to fabricate a variety of devices such as CO sensors, spin filters, oscillators, and amplifiers.

References

- [1] Andre K Geim and Konstantin S Novoselov. The rise of graphene. *Nat. Mater.*, 6:183–191, 2010.
- [2] Subhajit Biswas, Soumitra Kar, Tandra Ghoshal, Vishal D Ashok, Supriya Chakrabarti, and Subhadra Chaudhuri. Fabrication of GaN nanowires and nanoribbons by a catalyst assisted vapor–liquid–solid process. *Mater. Res. Bull.*, 42:428–436, 2007.
- [3] P Tsipas, S Kassavetis, D Tsoutsou, E Xenogiannopoulou, E Golias, SA Giamini, C Grazianetti, D Chiappe, A Molle, M Fanciulli, and A Dimoulas. Evidence for graphite-like hexagonal AlN nanosheets epitaxially grown on single crystal Ag (111). *Appl. Phys. Lett.*, 103:251605–1–251605–4, 2013.
- [4] Suchismita Ghosh, Wenzhong Bao, Denis L Nika, Samia Subrina, Evghenii P Pokatilov, Chun Ning Lau, and Alexander A Balandin. Dimensional crossover of thermal transport in few-layer graphene. *Nat. Mater.*, 9:555–558, 2010.
- [5] Ali Ahmadi Peyghan, Somayeh F Rastegar, and Nasser L Hadipour. DFT study of NH₃ adsorption on pristine, Ni-and Si-doped graphynes. *Phys. Lett. A*, 378:2184–2190, 2014.

- [6] Hyeun Joong Yoon, Do Han Jun, Jin Ho Yang, Zhixian Zhou, Sang Sik Yang, and Mark Ming-Cheng Cheng. Carbon dioxide gas sensor using a graphene sheet. *Sens. Actuators, B*, 157:310–313, 2011.
- [7] Marjaneh Samadizadeh, Ali Ahmadi Peyghan, and Somayeh F Rastegar. Sensing behavior of BN nanosheet toward nitrous oxide: a DFT study. *Chin. Chem. Lett.*, 26:1042–1045, 2015.
- [8] Bing Huang, Zuanyi Li, Zhirong Liu, Gang Zhou, Shaogang Hao, Jian Wu, Bing-Lin Gu, and Wenhui Duan. Adsorption of gas molecules on graphene nanoribbons and its implication for nanoscale molecule sensor. *J. Phys. Chem. C*, 112:13442–13446, 2008.
- [9] Md Monirojjaman Monshi, Sadegh Mehdi Aghaei, and Irene Calizo. Doping and defect-induced germanene: a superior media for sensing H_2S , SO_2 , and CO_2 gas molecules. *Surf. Sci.*, 665:96–102, 2017.
- [10] Rachana Yogi and Neeraj K Jaiswal. First-principle study of NO_2 adsorption and detection on the edges of zigzag nitride nanoribbons. *Physica E*, 114:113575–113587, 2019.
- [11] R González-Ariza, O Martínez-Castro, María G Moreno-Armenta, A Gonzalez-Garcia, W Lopez-Perez, and R Gonzalez-Hernandez. Tuning the electronic and magnetic properties of 2D g-GaN by H adsorption: An ab-initio study. *Physica B*, 569:57–61, 2019.
- [12] Zhen Cui, Kaifei Bai, Xia Wang, Enling Li, and Jiangshan Zheng. Electronic, magnetism, and optical properties of transition metals adsorbed g-GaN. *Physica E*, 118:113871, 2020.
- [13] Gang Xiao, Ling-Ling Wang, Qing-Yan Rong, Hai-Qing Xu, and Wen-Zhi Xiao. A comparative study on magnetic properties of Mo doped AlN, GaN and InN monolayers from first-principles. *Physica B*, 524:47–52, 2017.
- [14] Yunxu Chen, Jinxin Liu, Keli Liu, Jingjing Si, Yiran Ding, Linyang Li, Tianrui Lv, Jianping Liu, and Lei Fu. GaN in different dimensionalities: Properties, synthesis, and applications. *Mater. Sci. Eng., R*, 138:60–84, 2019.
- [15] Zhaoyong Guan and Shuang Ni. Prediction of high curie temperature, large magnetic crystal anisotropy, and carrier doping-induced half-metallicity in two-dimensional ferromagnetic FeX_3 ($\text{X} = \text{F}, \text{Cl}, \text{Br}, \text{and I}$) monolayers. *J. Phys. Chem. C*, 125:16700–16710, 2021.
- [16] Yi Luo, Chongdan Ren, Yujing Xu, Jin Yu, Sake Wang, and Minglei Sun. A first principles investigation on the structural, mechanical, electronic, and catalytic properties of biphenylene. *Sci. Rep.*, 11:1–6, 2021.
- [17] Minglei Sun, Yi Luo, Yuan Yan, and Udo Schwingenschlogl. Ultrahigh carrier mobility in the two-dimensional semiconductors B_8Si_4 , B_8Ge_4 , and B_8Sn_4 . *Chem. Mater.*, 33:6475–6483, 2021.
- [18] Zhen Cui, Yi Luo, Jin Yu, and Yujing Xu. Tuning the electronic properties of MoSi_2N_4 by molecular doping: a first principles investigation. *Physica E*, 134:114873–114880, 2021.
- [19] Zhaoyong Guan and Shuang Ni. Strain-controllable high curie temperature, large valley polarization, and magnetic crystal anisotropy in a 2D ferromagnetic janus VSeTe monolayer. *ACS Appl. Mater. Interfaces*, 12:53067–53075, 2020.
- [20] Hidefumi Hiura. Tailoring graphite layers by scanning tunneling microscopy. *Appl. Surf. Sci.*, 222:374–381, 2004.
- [21] Urmimala Maitra, HSS Matte, Prashant Kumar, and CNR Rao. Strategies for the synthesis of graphene, graphene nanoribbons, nanoscrolls and related materials. *Chimia*, 66:941–948, 2012.
- [22] Claire Berger, Zhimin Song, Xuebin Li, Xiaosong Wu, Nate Brown, Cécile Naud, Didier Mayou, Tianbo Li, Joanna Hass, Alexei N Marchenkov, Edward H Conrad, Phillip N First, and Walt A. de Heer. Electronic confinement and coherence in patterned epitaxial graphene. *Science*, 312:1191–1196, 2006.
- [23] Claire Berger, Zhimin Song, Tianbo Li, Xuebin Li, Asmerom Y Ogbazghi, Rui Feng, Zhenting Dai, Alexei N Marchenkov, Edward H Conrad, Phillip N First, and Walt A. de Heer. Ultrathin epitaxial graphite: 2D electron gas properties and a route toward graphene-based nanoelectronics. *J. Phys. Chem. B*, 108:19912–19916, 2004.

- [24] Xiaoting Jia, Mario Hofmann, Vincent Meunier, Bobby G Sumpter, Jessica Campos-Delgado, José Manuel Romo-Herrera, Hyungbin Son, Ya-Ping Hsieh, Alfonso Reina, Jing Kong, Mauricio Terrones, and Mildred S Dresselhaus. Controlled formation of sharp zigzag and armchair edges in graphitic nanoribbons. *Science*, 323:1701–1705, 2009.
- [25] Mitsutaka Fujita, Katsunori Wakabayashi, Kyoko Nakada, and Koichi Kusakabe. Peculiar localized state at zigzag graphite edge. *J. Phys. Soc. Japan*, 65:1920–1923, 1996.
- [26] Kyoko Nakada, Mitsutaka Fujita, Gene Dresselhaus, and Mildred S Dresselhaus. Edge state in graphene ribbons: Nanometer size effect and edge shape dependence. *Phys. Rev. B*, 54:17954–17962, 1996.
- [27] Qing Tang, Yao Cui, Yafei Li, Zhen Zhou, and Zhongfang Chen. How do surface and edge effects alter the electronic properties of GaN nanoribbons? *J. Phys. Chem. C*, 115:1724–1731, 2011.
- [28] Motohiko Ezawa. Peculiar width dependence of the electronic properties of carbon nanoribbons. *Phys. Rev. B*, 73:045432–045441, 2006.
- [29] Kyle A Ritter and Joseph W Lyding. The influence of edge structure on the electronic properties of graphene quantum dots and nanoribbons. *Nat. Mater.*, 8:235–242, 2009.
- [30] Haiming Li, Jun Dai, Jiong Li, Shuo Zhang, Jing Zhou, Linjuan Zhang, Wangsheng Chu, Dongliang Chen, Haifeng Zhao, Jinlong Yang, and Ziyu Wu. Electronic structures and magnetic properties of GaN sheets and nanoribbons. *J. Phys. Chem. C*, 114:11390–11394, 2010.
- [31] Zhen Wah Tan, Jian-Sheng Wang, and Chee Kwan Gan. First-principles study of heat transport properties of graphene nanoribbons. *Nano Lett.*, 11:214–219, 2011.
- [32] AJ Du, Sean C Smith, and GQ Lu. First-principle studies of electronic structure and C-doping effect in boron nitride nanoribbon. *Chem. Phys. Lett.*, 447:181–186, 2007.
- [33] Seung Yong Bae, Hee Won Seo, Jeunghye Park, Hyunik Yang, and Se Ahn Song. Synthesis and structure of gallium nitride nanobelts. *Chem. Phys. Lett.*, 365:525–529, 2002.
- [34] Li Yang, Xing Zhang, Ru Huang, Guoyan Zhang, and Xia An. Synthesis of single crystalline GaN nanoribbons on sapphire (0001) substrates. *Solid State Commun.*, 130:769–772, 2004.
- [35] KC Lo, HP Ho, PK Chu, and KW Cheah. Synthesis of gallium nitride film and gallium oxide nano-ribbons by plasma immersion ion implantation of nitrogen into gallium arsenide. pages 132–136, 2003.
- [36] Fang-Ling Zheng, Yan Zhang, Jian-Min Zhang, and Ke-Wei Xu. Structural, electronic, and magnetic properties of C-doped GaN nanoribbon. *J. Appl. Phys.*, 109:104313, 2011.
- [37] Xinyan Xia, Shiyong Guo, Lili Xu, Tingting Guo, Zhenhua Wu, and Shengli Zhang. Sensing performance of SO₂, SO₃ and NO₂ gas molecules on 2D pentagonal PdSe₂: A first-principle study. *IEEE Electron Device Lett.*, 42:573–576, 2021.
- [38] Hareem Khan, Ali Zavabeti, Jian Zhen Ou, Torben Daeneke, YongXiang Li, and Kourosh Kalantar-zadeh. Two dimensional tungsten oxide nanosheets with unprecedented selectivity and sensitivity to NO₂. pages 1–3, 2017.
- [39] Zhen Cui, Xia Wang, Yingchun Ding, Enling Li, Kaifei Bai, Jiangshan Zheng, and Tong Liu. Adsorption of CO, NH₃, NO, and NO₂ on pristine and defective g-GaN: improved gas sensing and functionalization. *Appl. Surf. Sci.*, 530:147275–147275, 2020.
- [40] Pengfei Wu, Zhen Cui, Qi Li, and Yingchun Ding. Gas (CO and NO) adsorption and sensing based on transition metals functionalized janus mosse. *Appl. Surf. Sci.*, 565:150509–1–150509–13, 2021.
- [41] Guo-Xiang Chen, Han-Fei Li, Dou-Dou Wang, Si-Qi Li, Xiao-Bo Fan, and Jian-Min Zhang. Adsorption of toxic gas molecules on pristine and transition metal doped hexagonal GaN monolayer: A first-principles study. *Vacuum*, 165:35–45, 2019.
- [42] Rachana Yogi, Neeraj K Jaiswal, and Pankaj Srivastava. First-principles study of sensing SO₂ adsorption on III-V nitride nanoribbons. *Mater. Chem. Phys.*, 242:122437, 2020.

- [43] Melinda Y Han, Barbaros Özyilmaz, Yuanbo Zhang, and Philip Kim. Energy band-gap engineering of graphene nanoribbons. *Phys. Rev. Lett.*, 98:206805–206812, 2007.
- [44] Young-Woo Son, Marvin L Cohen, and Steven G Louie. Energy gaps in graphene nanoribbons. *Phys. Rev. Lett.*, 97:216803–216807, 2006.
- [45] Mads Brandbyge, José-Luis Mozos, Pablo Ordejón, Jeremy Taylor, and Kurt Stokbro. Density-functional method for nonequilibrium electron transport. *Phys. Rev. B*, 65:165401–1–165401–17, 2002.
- [46] John P Perdew, Kieron Burke, and Matthias Ernzerhof. Generalized gradient approximation made simple. *Phys. Rev. Lett.*, 77:3865–3868, 1996.
- [47] Hendrik J Monkhorst and James D Pack. Special points for Brillouin-zone integrations. *Phys. Rev. B*, 13:5188–5192, 1976.
- [48] LL Song, XH Zheng, H Hao, J Lan, XL Wang, and Z Zeng. Tuning the electronic and magnetic properties in zigzag boron nitride nanoribbons with carbon dopants. *Comput. Mater. Sci.*, 81:551–555, 2014.
- [49] Pankaj Srivastava, Varun Sharma, and Neeraj K Jaiswal. Adsorption of COCl_2 gas molecule on armchair boron nitride nanoribbons for nano sensor applications. *Microelectron. Eng.*, 146:62–67, 2015.
- [50] Hasan Şahin, Seymur Cahangirov, Mehmet Topsakal, E Bekaroglu, E Akturk, Ramazan Tuğrul Senger, and Salim Ciraci. Monolayer honeycomb structures of group-IV elements and III-V binary compounds: First-principles calculations. *Phys. Rev. B*, 80:155453–1–155453–12, 2009.
- [51] Jariyane Prasongkit, Vivekanand Shukla, Anton Grigoriev, Rajeev Ahuja, and Vittaya Amornkitbamrung. Ultrahigh-sensitive gas sensors based on doped phosphorene: A first-principles investigation. *Appl. Surf. Sci.*, 497:143660–143668, 2019.
- [52] GC Loh, Sandeep Nigam, G Mallick, and Ravindra Pandey. Carbon-doped boron nitride nanomesh: stability and electronic properties of adsorbed hydrogen and oxygen. *J. Phys. Chem. C*, 118:23888–23896, 2014.
- [53] Guodong Sun, Peng Zhao, Wenxue Zhang, Hui Li, and Cheng He. Adsorption of gas molecules on armchair AlN nanoribbons with a dangling bond defect by using density functional theory. *Mater. Chem. Phys.*, 186:305–311, 2017.
- [54] Sudhir Kumar, Manoj Singh, Durgesh Kumar Sharma, and Sushil Auluck. Enhancing gas adsorption properties of borophene by embedding transition metals. *Comput. Condens. Matter*, 22:e00436, 2020.
- [55] Werner Reckien, Florian Janetzko, Michael F Peintinger, and Thomas Bredow. Implementation of empirical dispersion corrections to density functional theory for periodic systems. *J. Comput. Chem.*, 33:2023–2031, 2012.
- [56] Niranjana V Ilawe, Jonathan A Zimmerman, and Bryan M Wong. Breaking badly: DFT-D2 gives sizeable errors for tensile strengths in palladium-hydride solids. *J. Chem. Theory Comput.*, 11:5426–5435, 2015.
- [57] Yurong Dai, Xiaojie Chen, and Chenghuan Jiang. Electronic structures of zigzag AlN, GaN nanoribbons and $\text{Al}_x\text{Ga}_{1-x}$ nanoribbon heterojunctions: First-principles study. *Physica B*, 407:515–518, 2012.
- [58] Neeraj K Jaiswal, Neha Tyagi, Amit Kumar, and Pankaj Srivastava. Inducing half-metallicity with enhanced stability in zigzag graphene nanoribbons via fluorine passivation. *Appl. Surf. Sci.*, 396:471–479, 2017.
- [59] Soubhik Chakrabarty, AHM Abdul Wasey, Ranjit Thapa, and GP Das. First principles design of divacancy defected graphene nanoribbon based rectifying and negative differential resistance device. *AIP Advances*, 5:087163–087174, 2015.
- [60] Nuala M Caffrey, Daniel Fritsch, Thomas Archer, Stefano Sanvito, and Claude Ederer. Spin-filtering efficiency of ferrimagnetic spinels CoFe_2O_4 and NiFe_2O_4 . *Phys. Rev. B*, 87:024419–1–024419–7, 2013.
- [61] Mubashir A Kharadi, Gul Faroz A Malik, Farooq A Khanday, and Khurshed A Shah. Hydrogenated silicene based magnetic junction with improved tunneling magnetoresistance and spin-filtering efficiency. *Phys. Lett. A*, 384:126826–1–126826–10, 2020.
- [62] Tong Chen, Chengkun Guo, Liang Xu, Quan Li, Kaiwu Luo, Desheng Liu, Lingling Wang, and Mengqiu Long. Modulating the properties of multi-functional molecular devices consisting of zigzag gallium nitride nanoribbons by different magnetic orderings: a first-principles study. *Phys. Chem. Chem. Phys.*, 20:5726–5733, 2018.